# Supporting Information

# Conformational dynamics in penicillin-binding protein 2a of methicillin-resistant *Staphylococcus aureus*, allosteric communication network and enablement of catalysis

Kiran V. Mahasenan[1], Rafael Molina[2], Renee Bouley[1], María T. Batuecas[2], Jed F. Fisher[1], Juan A. Hermoso[2], Mayland Chang[1], and Shahriar Mobashery[1,*]

[1]Department of Chemistry and Biochemistry, University of Notre Dame, Notre Dame, IN 46556, USA.
[2]Department of Crystallography and Structural Biology, Institute of Physical Chemistry "Rocasolano", CSIC, 28006 Madrid, Spain.

*S.M.: E-mail, mobashery@nd.edu; Phone, +1-574-631-2933

## Table of contents

**Table S1.** X-ray Data collection and refinement statistics.

| | PBP2a:cefepime | PBP2a:oxacilin | PBP2a:ceftazidime |
|---|---|---|---|
| **Data collection** | | | |
| Space group | $P2_12_12_1$ | $P2_12_12_1$ | $P2_12_12_1$ |
| Cell dimensions | | | |
| *a*, *b*, *c* (Å) | 80.62, 101.19, 186.62 | 80.50, 102.19, 185.68 | 80.74, 101.91, 186.45 |
| α, β, γ (°) | 90, 90, 90 | 90, 90, 90 | 90, 90, 90 |
| Wavelength | 1.0000 | 1.0000 | 1.0000 |
| Resolution (Å) | 186.62-1.98 (2.09-1.98)* | 49.07-2.00 (2.03-2.00)* | 101.91-2.00 (2.07-2.00)* |
| $R_{pim}$ | 0.04 (0.38) | 0.03 (0.21) | 0.03 (0.35) |
| CC(1/2) | 0.99 (0.89) | 0.99 (0.94) | 0.99 (0.89) |
| *Mean I* / σ(*I*) | 14.8 (2.2) | 13.1 (2.9) | 12.3 (2.2) |
| Completeness (%) | 93.8 (91.9) | 99.9 (99.8) | 97.8 (97.7) |
| Redundancy | 7.2 (7.1) | 5.1 (4.1) | 7.1 (7.5) |
| | | | |
| **Refinement** | | | |
| Resolution (Å) | 93.31-1.98 | 46.42-2.00 | 93.23-2.00 |
| No. Reflections | 100216 | 197867 | 101947 |
| $R_{work}$ / $R_{free}$ | 0.21/0.25 | 0.19/0.25 | 0.20/0.24 |
| No. Atoms | | | |
| Protein | 10291 | 10256 | 10254 |
| Ligands | 34 | 34 | 34 |
| Ions | 5 | 6 | 6 |
| Water | 440 | 663 | 420 |
| R.m.s. deviations | | | |
| Bond lengths (Å) | 0.008 | 0.007 | 0.008 |
| Bond angles (°) | 1.022 | 0.914 | 0.868 |
| **PDB code** | 5M18 | 5M19 | 5M1A |

*Values in parentheses are for highest-resolution shell. One crystal was used to solve each structure.

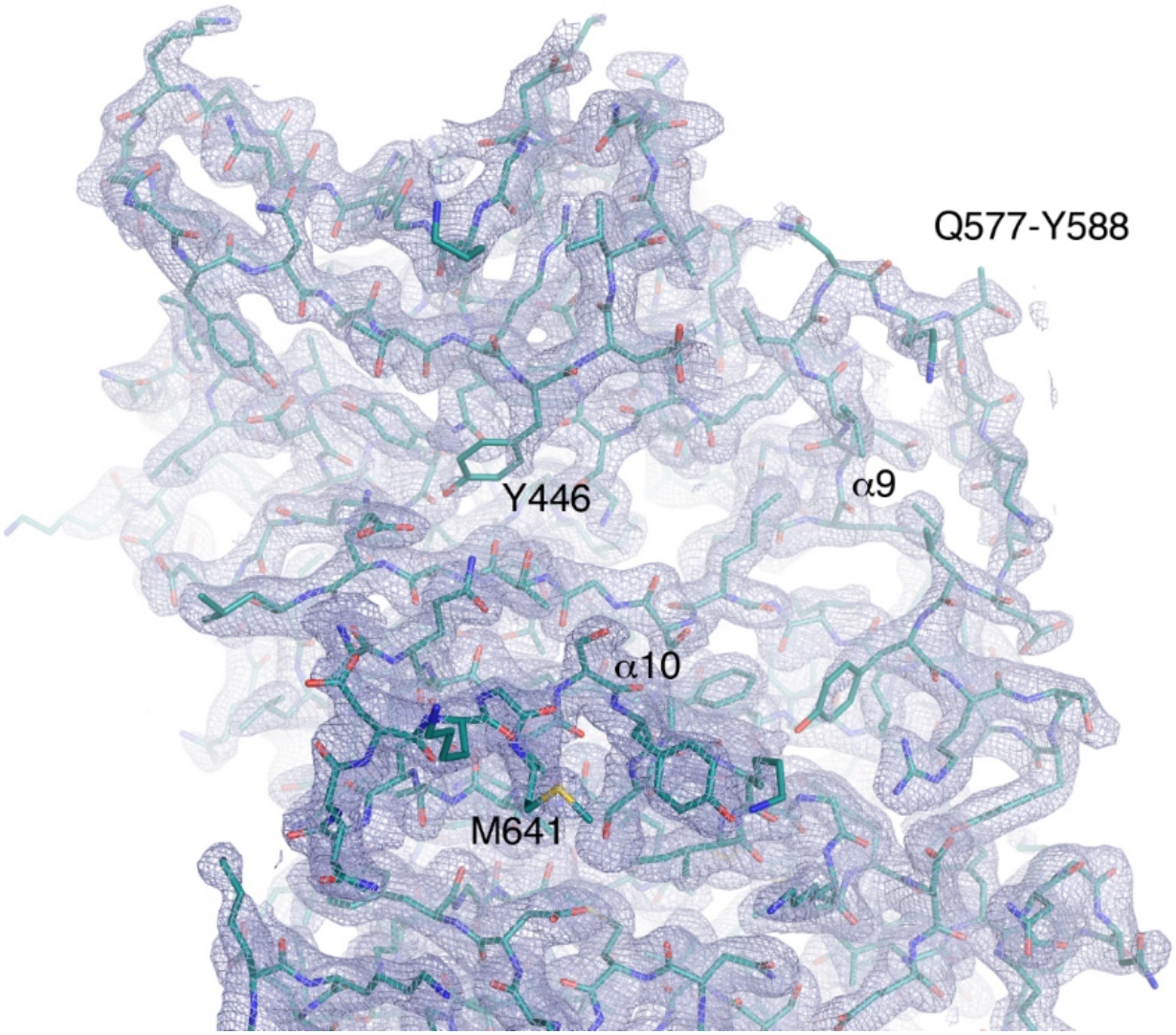


**Figure S1.** Electron-density map of the PBP2a:oxacillin complex. Partial view of the active site in the PBP2a:oxacillin complex (same perspective as in Figure 1B) with the protein represented as capped sticks. Regions presented changes are labelled (see text). The 2Fo-Fc map is contoured at 1σ.

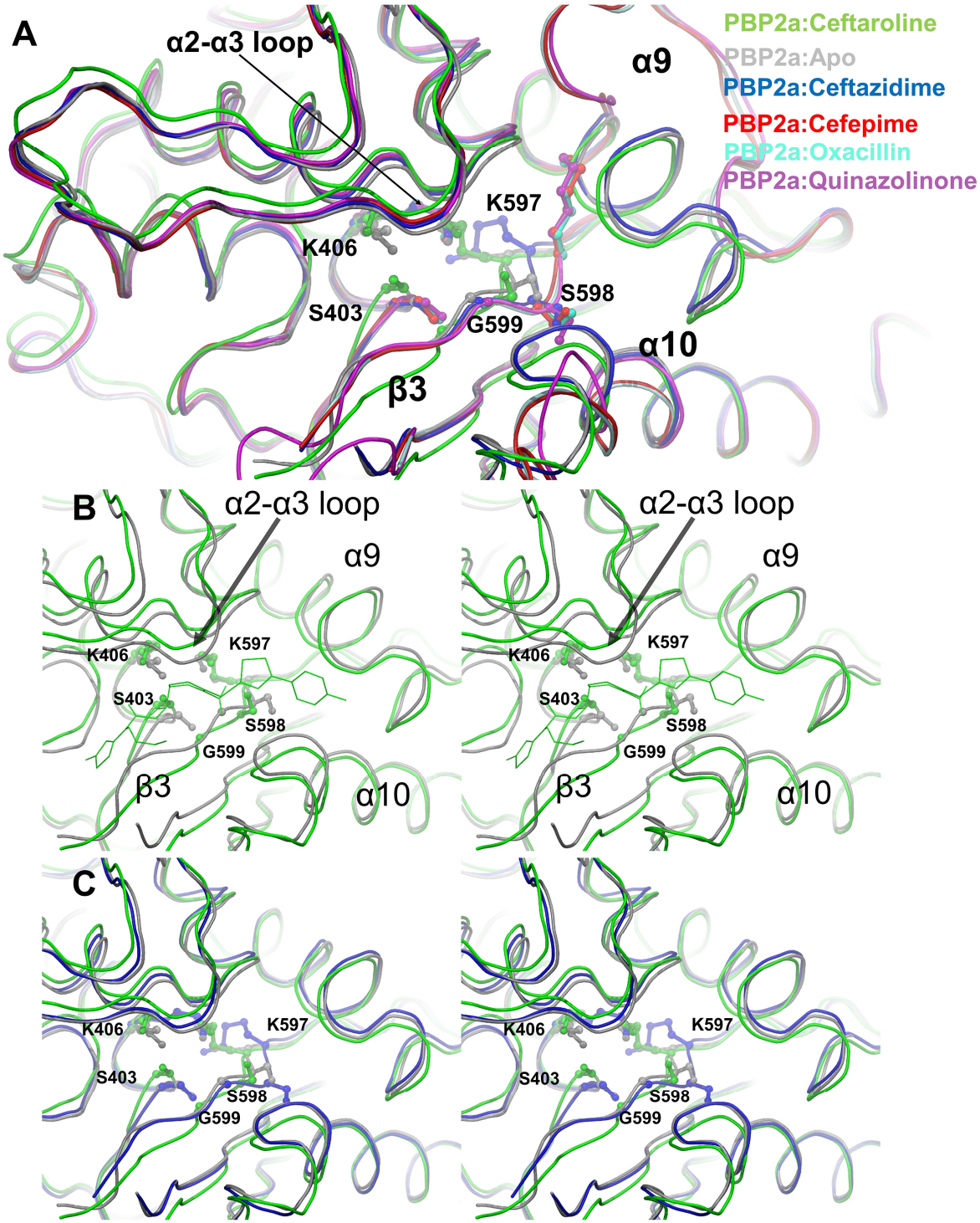


**Figure S2.** Structural changes observed at the active site of PBP2a in different β-lactam complexes. Images are in stereo, except for panel A (A) Superposition of all the X-ray crystal structures. (B) PBP2a:ceftaroline complex (PBD ID: 3ZG0, colored green)[1] superposed to apo crystal structure (PBD ID: 1VQQ, gray)[2]. Ceftaroline covalently bound to S403 is displayed as green line representation). (C) PBP2a:ceftazidime complex (blue; this work) superimposed to PBP2a:ceftaroline and apo structures. (Figure S2 continues in the following page).

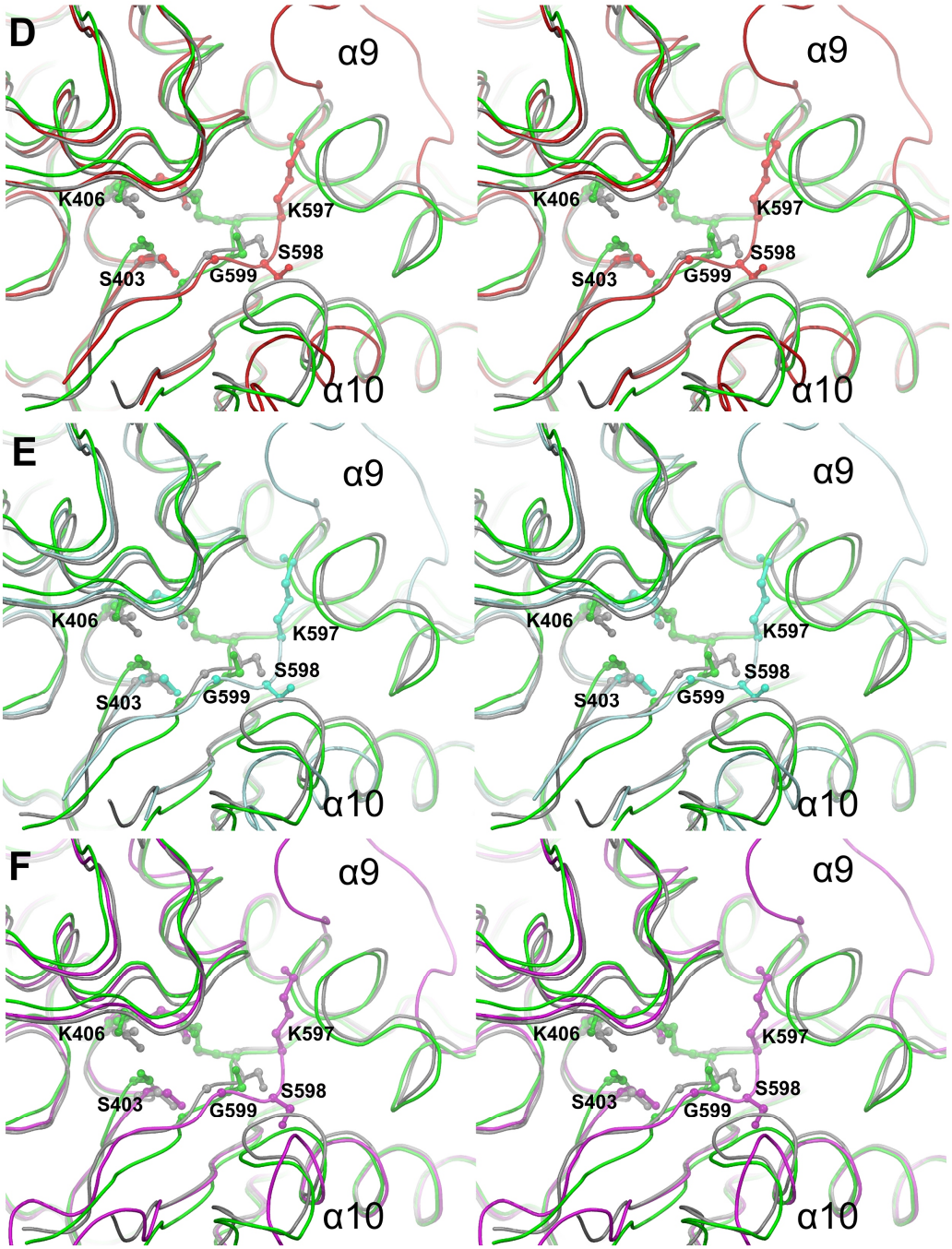


**Figure S2 (continued).** (D) PBP2a: cefepime complex (red; this work) superimposed to PBP2a:ceftaroline and apo structures. (E) PBP2a: oxacillin complex (aqua; this work) superimposed to PBP2a:ceftaroline and apo structures. (F) PBP2a:quinazolinone complex (PDB ID: 4CJN; purple)[3] superimposed to PBP2a:ceftaroline and apo structures. In the presence of ceftazidime (C, this work), cefepime (D, this work), oxacillin (E, this work) and quinazoline (F, PDB code 4CJN) at the allosteric site, relevant structural changes are observed for the α9, α10 and also in the β3 strand of the transpeptidase domain. Displacement of the β3 strand is observed for the three β-lactam complexes reported here (largest displacement observed for K597). The twist of β3 strand at the catalytic site, as observed in the X-ray structures of PBP2a:ceftaroline complex (B, as well as in other acylated PBP2a complexes), that moves G599 into contact with catalytic S403 is not observed in any of the complexes with the antibiotics bound only at the allosteric site.

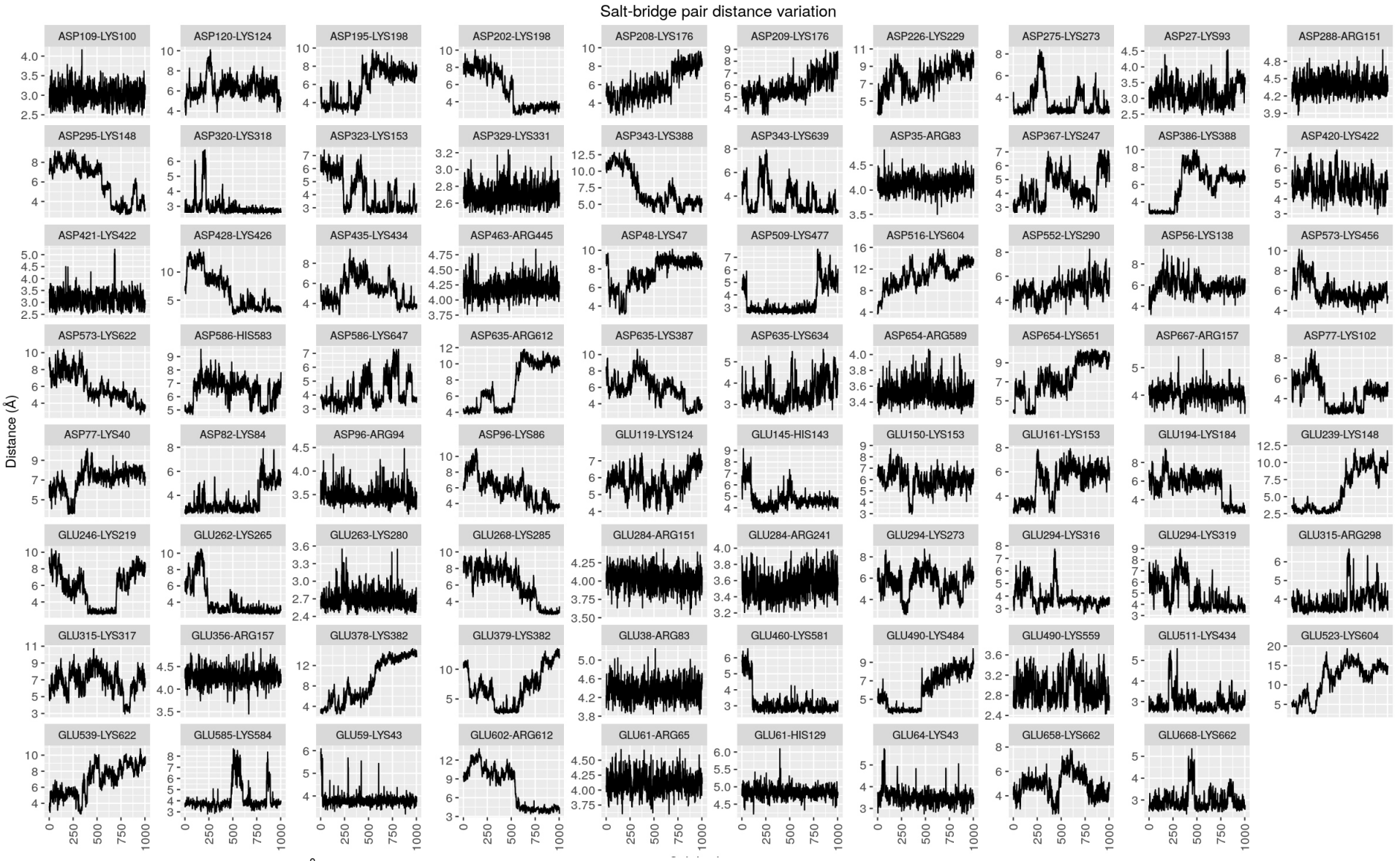


**Figure S3.** Salt-bridge distance (Å) variation during TMD simulated active-site opening, as sampled by 1000 snapshots (x-axis) of the trajectory.

**Table S2.** PBP2a X-ray structures used in the analysis of salt-bridge interactions and dynamic allosteric-residue calculations by the STRESS program

| ID | PDB ID | Chain | Ligand Name | Structure Title | Pub. Year | Journal Name | PMID |
|---|---|---|---|---|---|---|---|
| 1 | 1MWR | A | Apo | SeMet PBP2a from MRSA | 2002 | Nat.Struct.Mol.Biol. | 12389036 |
| 2 | 1MWR | B | Apo | SeMet PBP2a from MRSA | 2002 | Nat.Struct.Mol.Biol. | 12389036 |
| 3 | 1VQQ | A | Apo | PBP2a from MRSA | 2002 | Nat.Struct.Mol.Biol. | 12389036 |
| 4 | 1VQQ | B | Apo | PBP2a from MRSA | 2002 | Nat.Struct.Mol.Biol. | 12389036 |
| 5 | 4BL2 | A | Apo | PBP2a clinical mutant E150K from MRSA | 2014 | J.Am.Chem.Soc. | 24955778 |
| 6 | 4BL2 | B | Apo | PBP2a clinical mutant E150K from MRSA | 2014 | J.Am.Chem.Soc. | 24955778 |
| 7 | 4BL3 | A | Apo | PBP2a clinical mutant N146K from MRSA | 2014 | J.Am.Chem.Soc. | 24955778 |
| 8 | 4BL3 | B | Apo | PBP2a clinical mutant N146K from MRSA | 2014 | J.Am.Chem.Soc. | 24955778 |
| 9 | 4CPK | A | Apo | PBP2a double clinical mutant N146K-E150K from MRSA | 2014 | J.Am.Chem.Soc. | 24955778 |
| 10 | 4CPK | B | Apo | PBP2a double clinical mutant N146K-E150K from MRSA | 2014 | J.Am.Chem.Soc. | 24955778 |
| 11 | 1MWS | B | Apo | Nitrocefin acyl-PBP2a from MRSA strain 27r at 2.00 A resolution. | 2002 | Nat.Struct.Mol.Biol. | 12389036 |
| 12 | 3ZFZ | B | Apo | Ceftaroline acyl-PBP2a from MRSA with non- covalently bound ceftaroline and muramic acid at allosteric site obtained by soaking | 2013 | Proc.Natl.Acad.Sci. | 24085846 |
| 13 | 3ZG5 | B | Apo | PBP2a from MRSA in complex with peptidoglycan analogue at allosteric site | 2013 | Proc.Natl.Acad.Sci. | 24085846 |
| 14 | 4CJN | A | Apo | PBP2a from MRSA in complex with quinazolinone ligand | 2015 | J.Am.Chem.Soc. | 25629446 |
| 15 | 3ZG0 | A | ceftaroline + acyl | ceftaroline acyl-PBP2a from MRSA with non- covalently bound ceftaroline and muramic acid at allosteric site obtained by cocrystallization | 2013 | Proc.Natl.Acad.Sci. | 24085846 |
| 16 | 3ZG0 | B | ceftaroline + acyl | ceftaroline acyl-PBP2a from MRSA with non- covalently bound ceftaroline and muramic acid at allosteric site obtained by cocrystallization | 2013 | Proc.Natl.Acad.Sci | 24085846 |
| 17 | 3ZFZ | A | ceftaroline + acyl | ceftaroline acyl-PBP2a from MRSA with non- covalently bound ceftaroline and muramic acid at allosteric site obtained by soaking | 2013 | Proc.Natl.Acad.Sci. | 24085846 |
| 18 | 4DKI | A | Ceftobiprole | Structural Insights into the Anti- Methicillin-Resistant Staphylococcus aureus (MRSA) Activity of Ceftobiprole | 2012 | J.Biol.Chem. | 22815485 |
| 19 | 4DKI | B | Ceftobiprole | Structural Insights into the Anti- Methicillin-Resistant Staphylococcus aureus (MRSA) Activity of Ceftobiprole | 2012 | J.Biol.Chem. | 22815485 |
| 20 | 1MWT | A | penicillin G acyl | penicillin G acyl-PBP2a from MRSAstrain 27r at 2.45 A resolution. | 2002 | Nat.Struct.Mol.Biol. | 12389036 |
| 21 | 1MWT | B | penicillin G acyl | penicillin G acyl-PBP2a from MRSAstrain 27r at 2.45 A resolution. | 2002 | Nat.Struct.Mol.Biol. | 12389036 |
| 22 | 1MWU | A | methicillin acyl | methicillin acyl-PBP2a from MRSAstrain 27r at 2.60 A resolution. | 2002 | Nat.Struct.Mol.Biol. | 12389036 |
| 23 | 3ZG5 | A | allosterioc peptidoglycan analogue | PBP2a from MRSA in complex with peptidoglycan analogue at allosteric | 2013 | Proc.Natl.Acad.Sci. | 24085846 |
| 24 | 4CJN | B | allosteric quinazolinone | PBP2a from MRSA in complex with quinazolinone ligand | 2015 | J.Am.Chem.Soc. | 25629446 |

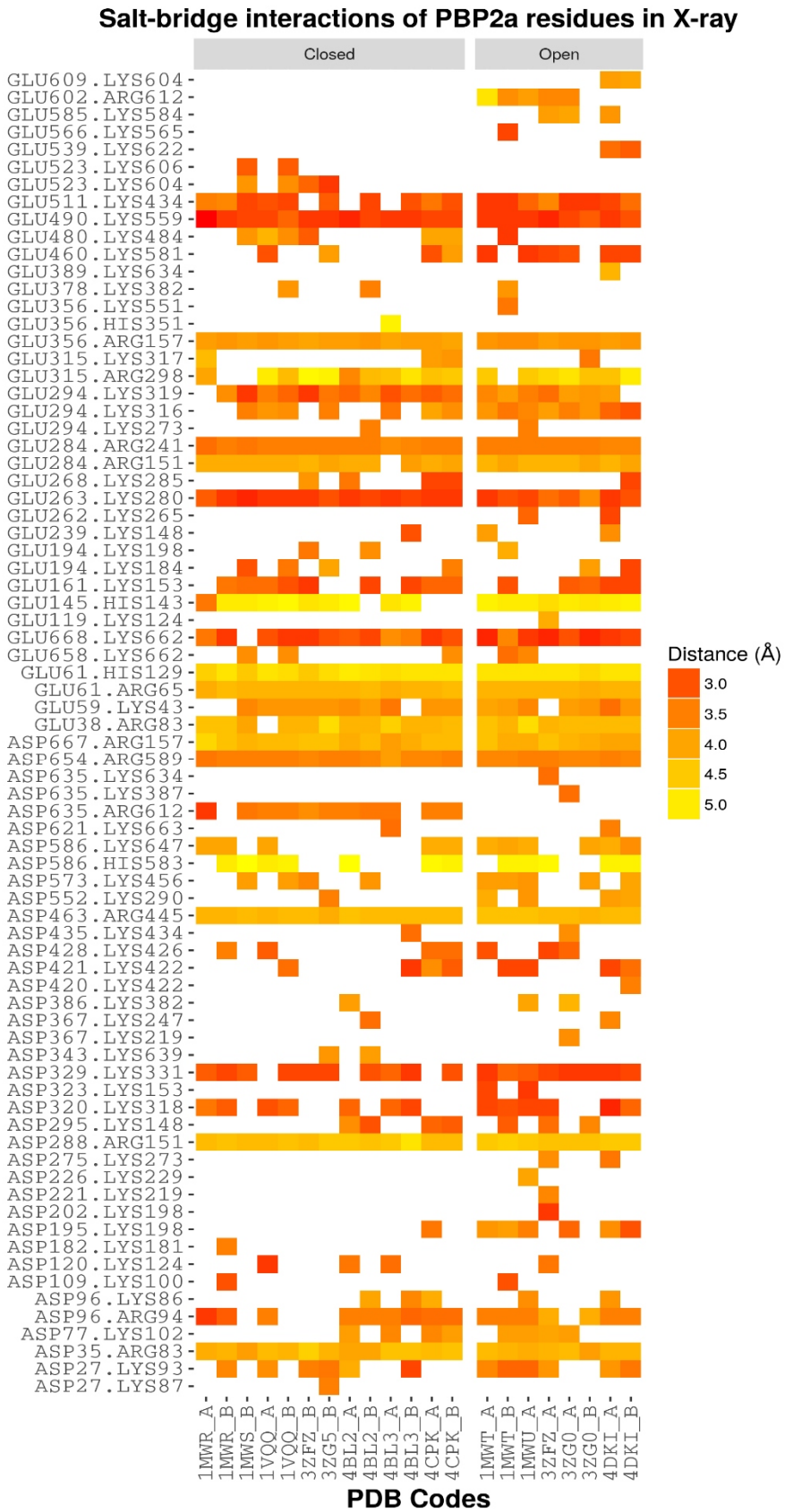


**Figure S4.** Heatmap of salt-bridge distances in the open and closed X-ray crystal structures listed in Table S2.

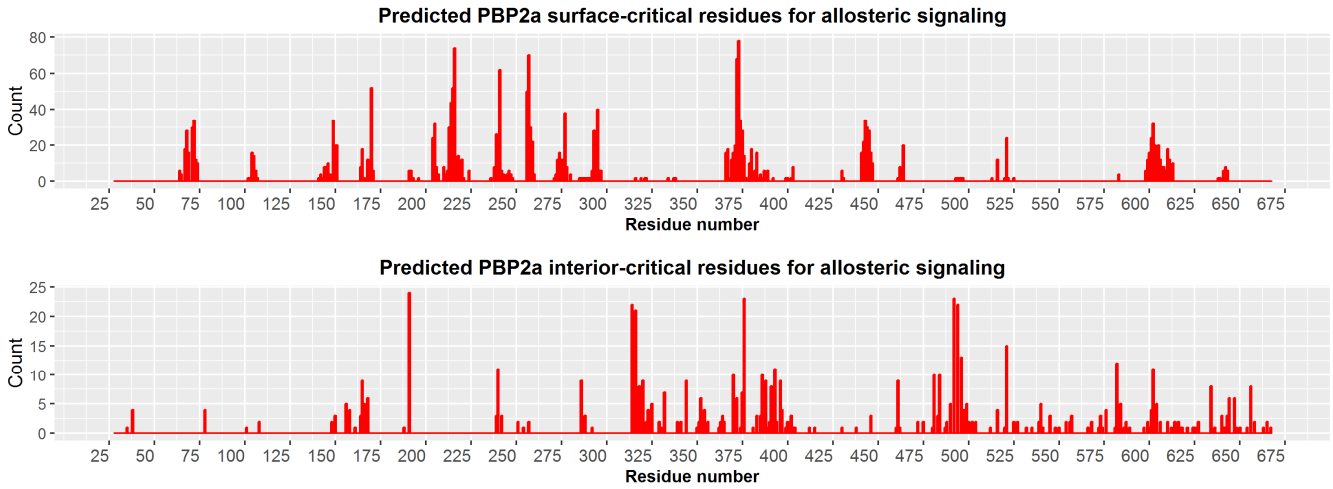


**Figure S5.** Predicted surface-critical and interior-critical residues from STRESS calculations. X-axis represent frequency of occurrence of the residues from the 24 independent calculations, each from a different X-ray structure monomer chain. Residues of the top-ranked five predicted sites for each X-ray structure were kept for the analysis for surface-critical residues.

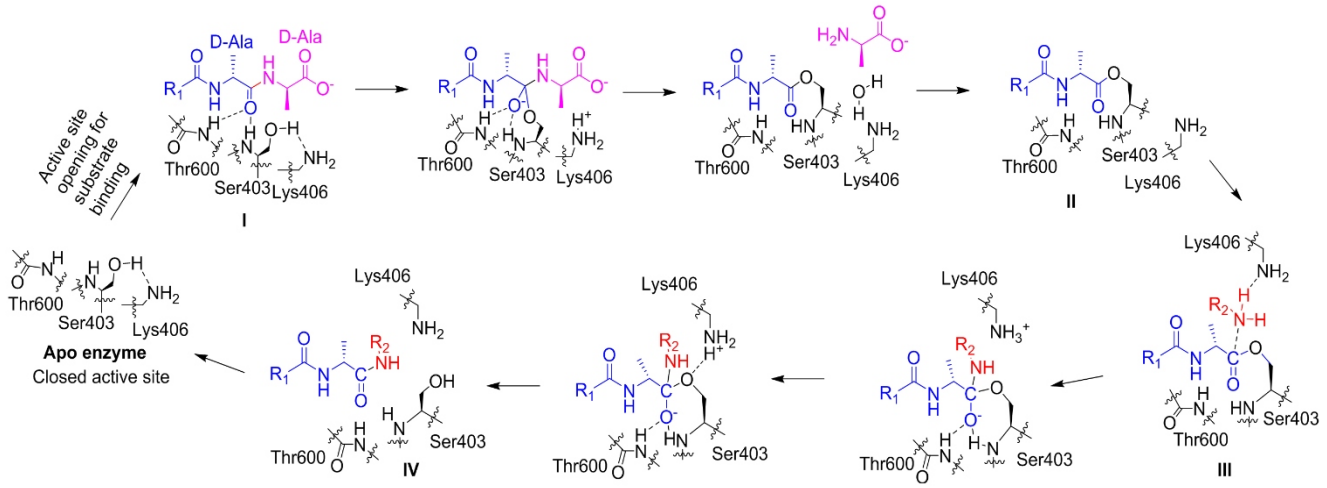


**Figure S6.** Enzymatic reaction events in the catalytic cycle of PBP2a based on previous QM/MM calculation of *S. pneumoniae* PBP1b.[4] Species I, II, III, and IV, which are labeled in the scheme, were modeled in the present study.

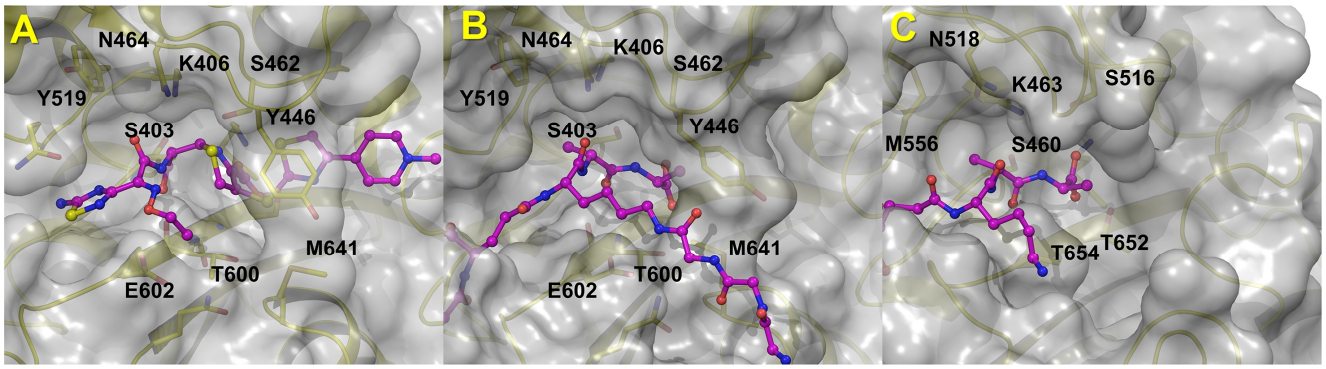


**Figure S7.** Binding interactions of the peptidoglycan and antibiotics with the active site of PBPs (A) *S. aureus* PBP2a (translucent gray surface representation) acylated by ceftaroline (purple for carbon atoms in ball and stick representation).[1] (B) Model of *S. aureus* PBP2a-peptidoglycan complex (species I, pre-acylation complex of PBP2a with PG1) from this study. (C) *S. pneumoniae* PBP1b-peptidoglycan complex evaluated in the previous QM/MM study.[4]

## REFERENCES

(1) Otero, L. H.; Rojas-Altuve, A.; Llarrull, L. I.; Carrasco-Lopez, C.; Kumarasiri, M.; Lastochkin, E.; Fishovitz, J.; Dawley, M.; Hesek, D.; Lee, M.; Johnson, J. W.; Fisher, J. F.; Chang, M.; Mobashery, S.; Hermoso, J. A. *Proc. Natl. Acad. Sci. U.S.A.* **2013**, *110*, 16808.

(2) Lim, D.; Strynadka, N. C. *Nat. Struct. Biol.* **2002**, *9*, 870.

(3) Bouley, R.; Kumarasiri, M.; Peng, Z.; Otero, L. H.; Song, W.; Suckow, M. A.; Schroeder, V. A.; Wolter, W. R.; Lastochkin, E.; Antunes, N. T.; Pi, H.; Vakulenko, S.; Hermoso, J. A.; Chang, M.; Mobashery, S. *J. Am. Chem. Soc.* **2015**, *137*, 1738.

(4) Shi, Q.; Meroueh, S. O.; Fisher, J. F.; Mobashery, S. *J. Am. Chem. Soc.* **2011**, *133*, 5274.